Dragging excitation characteristics from thermoelectric power in $Bi_2(Sr_{2-y}La_y)CuO_{6+\delta}$ single crystals

Y. Dumont*
Département de Physique, Université de Versailles St. Quentin, 45 Avenue des Etats-Unis, 78035 Versailles, France and CEA, Service de Physique de l'Etat Condensé, CE Saclay, 91191 Gif sur Yvette, France

C. Ayache
CEA, Service de Physique de l'Etat Condensé, CE Saclay, 91191 Gif sur Yvette, France

G. Collin
Laboratoire Léon Brillouin, CEA-CNRS, CE Saclay, 91191 Gif sur Yvette, France
(Received 20 August 1999; revised manuscript received 9 February 2000)

The *ab*-plane thermoelectric power (S) of Bi-2201 single crystals is used to establish the superconducting phase diagram that shows two branches, one matching the general curve for cuprates and a singular one, apparently linked to structural disorder. The low maximum T_c of 18 K allows us to follow the sequence $S(T)$ curves over a large absolute temperature range in the normal state for both the under- and overdoped regions. The results support a drag mechanism. A simplified model is used to make a quantitative characterization of the dragging excitations through their effective number of modes as well as the temperature dependence of their specific heat. This analysis points out relations between the phase diagram and the spectral shift and rearrangement of the excitation modes.

Obertelli, Cooper, and Tallon (OCT)[1–3] have empirically evidenced a remarkable property of the thermoelectric power (TEP, S) in high-temperature superconductors. For most of them, the room temperature value S_{290K} is independent of the considered cuprate, of the number of CuO_2 planes or of the chemical composition. Instead, it is univocally linked to the number of holes (p) injected in CuO_2 layers. The one-to-one correspondence has a clear practical interest as it provides an estimate of the p changes which follow cationic substitution or oxygen treatment. Departures from the generic OCT trend have been observed, however, and $La_{2-x}Sr_xCuO_4$, for instance, follows its own $S_{290K}(p)$ dependence.[3]

The origin of the empirical ''OCT law'' remains unclear, though several explanations have been proposed to explain the temperature and doping dependencies of the TEP in cuprates. Most models (narrow-band effects,[3–5] polaronic contribution[6]) are based on a pure charge-carrier diffusion mechanism but some refer to the phonons, which drag the charge carriers with them along the thermal gradient (see, e.g., Ref. 7). To clarify the debate, it is of interest to examine the normal state $S(T)$ dependence in a low-temperature range, usually masked by the onset of superconductivity. In this respect, the single-layer Bi-2201 is one of the best candidates owing to its low T_c^{max} value and to the possibility of doping it over the full range of the under- to overdoped regimes.[8] However, in carrying out experiments on this compound, care must be taken regarding the intensively modulated superstructure[9] and possibly related biasing effects. This is done in the present experimental study, which is made on a series of single crystals prepared at different doping levels. Using single crystals allows a structural follow up of both average and superstructure parameters in correlation with macroscopic evolutions. The T_c vs S_{290K} phase diagram is first established. Then, the set of $S(T)$ curves is examined and found phenomenologically to match a drag mechanism. On these grounds, a simplified model is proposed to characterize the dragging excitations by their effective number of modes and specific heat.

Doping is achieved by two means : La substitution on the Sr site and reversible annealing under air at various temperatures (T_{an}) between 350 °C, the crystal optimizing treatment,[10] and 680 °C. Crystals synthesis,[11] cationic stoichiometry determination,[11,12] and annealing effects on resistivity[10] and structure[11,13] are described elsewhere. The TEP is measured in the *ab* plane by an ac method using chromel constantan on samples of typical size $1-2\times0.5\times0.05$ mm^3. T_c is taken at midheight of the resistive transition. Electron-probe-micro-analysis gives the stoichiometric formula: $Bi_{2.1}(Sr_{1.9-y_{La}}La_{y_{La}})CuO_{6+\delta}$.[11,12] Crystal structure is followed using a four-circle x-ray diffractometer. The crystallographic phase diagram versus y_{La}, the level of La substitution, shows a structural change from a monoclinic (M) average structure for $y_{La}\leqslant0.27$ towards an orthorhombic (O) one above 0.45. Both structures are in fact modulated and the component q_{c*} of the superstructure wave vector, originally incommensurate in the M phase, locks-in in the O phase. Moreover, the change between M and O is not sudden but, as evidenced by microcrystallite studies, a coexistence region ($0.27\leqslant y_{La}\leqslant0.45$) exists in which diffraction lines of both phases look intricately mixed at a submicronic scale.[11,14] Nevertheless, this average structure mixing is not removed by a $T_{an}=680$ °C treatment, which was otherwise shown to induce disorder in the modulated structure along the c direction.[13]

In Fig. 1, the doping effect on superconductivity is shown by plotting T_c as a function of S_{290K}. In all cases, increasing

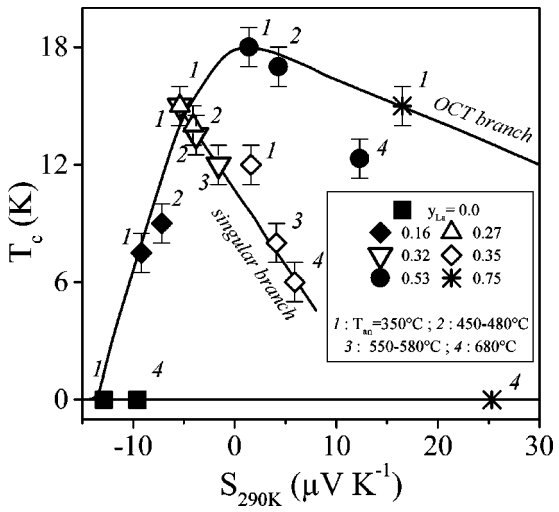

FIG. 1. Superconducting phase diagram resulting from La/Sr substitution and thermal annealing in $Bi_{2.1}(Sr_{1.9-y_{La}}La_{y_{La}})CuO_{6+\delta}$. T_c is plotted as a function of S_{290K} for different lanthanum substitutions (y_{La}) and annealing temperatures (T_{an}). The symbols relate to y_{La}, italic numbers labeling different T_{an} (see inset). The ''OCT branch'' indicates the part of the diagram that fits the generic OCT dependence scaled to $T_c^{max}=18$ K. Open symbols mark the ''mixed'' crystalline range that departs from the OCT behavior, most data regrouping along a ''singular branch.''

T_{an}, as well as y_{La}, generates an increased S_{290K} which means an underdoping trend for both parameters. The resulting phase diagram reveals a complex structure that can be clarified by comparing three annealing stages and by taking the different crystalline ranges into account. Considering first the $T_{an}=350\,°C$ ''optimal annealing stage'' (label 1 in Fig. 1), a fair agreement is obtained with the OCT generic curve provided T_c^{max} is set to 18 K (''OCT branch''). The lanthanum-free sample is nonsuperconducting and lies at the limit of the fully overdoped metallic range, whereas T_c^{max} occurs for $y_{La}\simeq 0.53$. A single concentration, $y_{La}=0.35$, (in the mixed range) lays off the OCT curve with $T_c=12$ K instead of the expected $T_c=18$ K. Now, increasing T_{an}, two distinct evolutions are evidenced for ''moderate annealing stage'' (labels 2 and 3 in Fig. 1). For La concentrations outside the mixed-crystalline region ($y_{La}=0.16,\ 0.53$), the upward or downward shifts observed in T_c conform to the trend expected from the OCT branch. However, inside the mixed-crystalline range ($y_{La}=0.27,\ 0.32,\ 0.35$; open symbols in Fig. 1), observed behavior markedly departs from OCT and T_c is systematically decreased as S_{290K} increases, thus generating a new branch. Finally, the annealing stage at 680 °C (label 4 in Fig. 1) induces a severe effect on superconductivity outside the mixed range: For $y_{La}=0.75$, T_c drops to zero instead of the expected 12 K while the lanthanum-free sample ($y_{La}=0$) does not become superconducting as OCT would predict. In the mixed-crystalline range, instead, $T_{an}=680\,°C$ shows no difference with moderate annealing treatments. In summary, the above results evidence two main branches in the superconducting phase diagram of Bi-2201 as established by the OCT method: the first branch matches the OCT generic regime and makes Bi-2201 similar to other cuprates despite the low T_c^{max} value; the second one, for which T_c rapidly drops with underdoping, is apparently

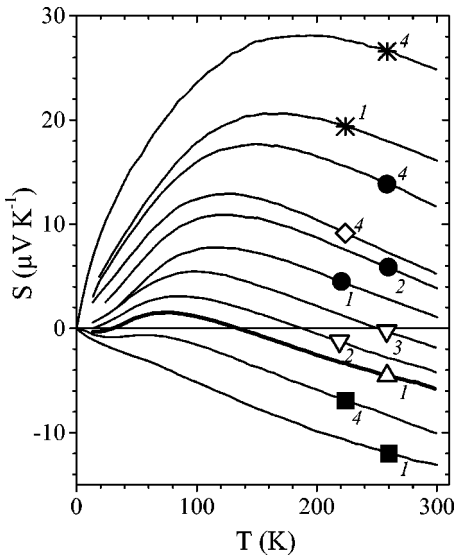

FIG. 2. *ab*-plane TEP versus temperature for $Bi_{2.1}(Sr_{1.9-y_{La}}La_{y_{La}})CuO_{6+\delta}$ single crystals. The symbols and labels are the same as in Fig. 1. For clarity, superposing curves and data below T_c are omitted. Heavy line marks the ($y_{La}=0.27$; $T_{an}=350\,°C$) sample for which $S(T)$ crosses the zero line twice.

linked to the mixed-crystalline phase occurring for $0.27\leqslant y_{La}\leqslant 0.45$. The superstructure disorder introduced by the 680 °C annealing does not alter the behavior of the mixed-phase specimens that describe the second branch, whereas it suppresses superconductivity for the other specimens and leads to departures from the OCT behavior. The T_c vs p diagram now follows with, especially, the bell shape reflecting the generic OCT curve (see dotted lines in Fig. 3).

As shown in Fig. 2, consider now, in the normal state, the full T dependence of TEP for different y_{La} and T_{an} values. Present behaviors are similar to the general trends observed in other cuprates[1,15] or Bi-2201 ceramics.[16,17] In the La-free sample, $S(T)$ is negative over the whole T range and close to

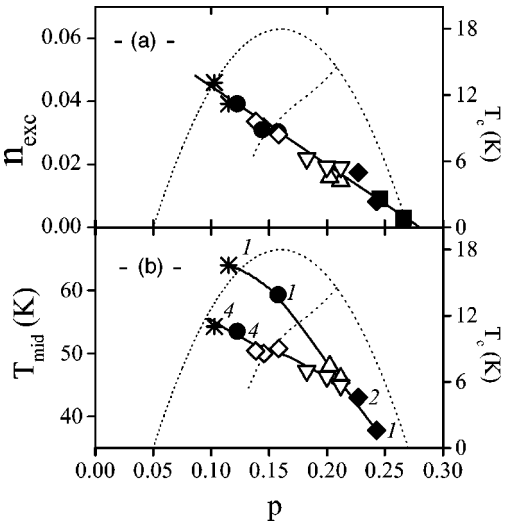

FIG. 3. n_{exc}, number of drag excitation modes, (a) and T_{mid} (b) versus p, the hole doping level. n_{exc} and p are referred to one CuO_2 unit. Same symbols and labels as in Fig. 1. Thin-dotted lines represent the superconducting phase diagram transposed from Fig. 1 (right-hand scale).

linear, a behavior also observed in overdoped non-superconducting Tl-2201.[1] On decreasing p, $S(T)$ acquires an oscillating aspect with a maximum shifting upwards and a low-T curvature evolving progressively from positive to negative. The oscillation may cross the zero line twice as for $y_{La}=0.27$, $T_{an}=350\,^{\circ}C$ (see also Refs. 16 and 17). Such behaviors would require an *ad hoc* hypothesis in a narrow-band picture to be explained but they are consistent with Trodhal's more simple view of a positive drag contribution added to the negative diffusion component.[7] The present $S(T)$ series indicates a moderately changing negative diffusion contribution superimposed on a more rapidly varying positive drag effect. As anticipated by Trodahl,[7] the latter retains basically a steplike form at all doping levels but the most heavily doped one, which marks an ultimate stage in the steady reduction of drag upon doping.

To further analyze this qualitative decomposition of S, let us introduce the following simplified model:[18]

$$S=S^{\mathrm{diff}}+S^{\mathrm{drag}}, \tag{1}$$

with

$$S^{\mathrm{diff}}=\frac{k_B}{e}\times a(T)\times T, \tag{2}$$

and

$$S^{\mathrm{drag}}=\frac{k_B}{e}\,\frac{n_{\mathrm{exc}}}{p}\,\frac{C^{*}_{\mathrm{exc}}(T)}{k_B}\,\frac{1/\tau_{\mathrm{exc\text{-}p}}}{1/\tau_{\mathrm{exc\text{-}p}}+1/\tau_{\mathrm{exc\text{-}other}}}, \tag{3}$$

with k_B the Boltzmann constant and e the electron charge. $a(T)$ in Eq. (2) is able to vary with T to account for possible narrow-band effects or for changes in the charge-carrier relaxation process. $C^{*}_{\mathrm{exc}}(T)$ in Eq. (3) represents the specific heat per mode of the hole dragging excitations. $C^{*}_{\mathrm{exc}}(T)$ is generally steplike and saturates at k_B. The step position can be characterized by the temperature at mid−height (T_{mid}) which also reflects the cutoff in the excitation energy spectrum. It provides a convenient means to distinguish between ''low'' and ''high'' temperature ranges ($T<$or$>2-3\times T_{\mathrm{mid}}$). The step shape reflects somehow the excitation energy spectrum. On the other hand, the last factor in the right-hand side of Eq. (3) represents the drag efficiency. This depends on the efficiency of excitation-hole scattering relative to all the other mechanisms (excitation-excitation, excitation-defects). When hole scattering dominates the total excitation relaxation rate ($1/\tau_{\mathrm{exc}}$), efficiency equals 1 and the T dependence of S^{drag} is entirely controlled by $C^{*}_{\mathrm{exc}}(T)$. Finally, the drag contribution strength is in general inversely proportional to p but, in addition, Eq. (3) introduces n_{exc}, an effective number of dragging excitation modes. In the present context, n_{exc} accounts for the possible evolution of the actual number of excitations with doping. Alternatively, its change may also indicate an unbalanced evolution linked to reciprocal space scattering geometry[7] or filtering effect due to strongly energy dependent scattering processes.[19] Then, the form of the step [and $C^{*}_{\mathrm{exc}}(T)$, as well] may incorporate the form of the filtering function, which puts a limit to our approximation.

Within the above scheme, consider first the high temperature (HT) range. For most doping levels, $S_{HT}(T)$ varies linearly, evidencing that $a(T)$ hardly changes with T and that $S^{\mathrm{drag}}_{HT}(T)\approx S^{\mathrm{drag}}_{0}$ (constant).[7] Thus, $S^{\mathrm{diff}}_{HT}(T)\approx-\alpha T$ and extrapolating $S_{HT}(T)\approx-\alpha T+S^{\mathrm{drag}}_{0}$ at $T=0$ allows a determination of S^{drag}_{0} and an estimate of $n_{\mathrm{exc}}[\equiv e/(k_B\times S^{\mathrm{drag}}_{0}\times p)]$. The changes of n_{exc} with p, resulting from such treatment, are shown in Fig. 3(a) and give a clear evidence: Irrespective of phase diagram features like the maximum at $T_c^{\max}$ or the existence of the singular branch, all data merge on a single decreasing curve. In the investigated doping range, this can be fitted linearly as $n_{\mathrm{exc}}=0.07-0.25\times p$ (per CuO_2 unit). This shows two important facts: (1) the effective drag excitation modes are in any case significantly less than the number of Cu sites and (2) n_{exc} vanishes for $p=0.28$, very close to $p_{c2}=0.27$, the upper critical concentration in the bell shape diagram. This questions a possible correlation between the onset of superconductivity and the existence of specific drag excitation modes. However, the absence of any difference between the bell shape and the singular branch also indicates that dragging excitations are not sufficient to generate the superconducting state by themselves. This is specially true for the La-free sample where the drag effect is generated by an annealing treatment at $T_{an}=680\,^{\circ}C$ but that remains not superconducting.

Further structure emerges from the low-temperature range in which $C^{*}_{\mathrm{exc}}(T)$, can be estimated. For that, assuming $S^{\mathrm{diff}}(T)=-\alpha T$ over the whole T range and subtracting from $S(T)$, one readily gets $C^{*}_{\mathrm{exc}}(T)/k_B\approx S^{\mathrm{drag}}(T)/S^{\mathrm{drag}}_{0}$. As stated above, two characteristics of $C^{*}_{\mathrm{exc}}(T)$ are the temperature at midheight of the step (T_{mid}) and the form of the step itself. Consider first the changes of $T_{\mathrm{mid}}(p)$ with p as shown in Fig. 3(b). In contrast with $n_{\mathrm{exc}}(p)$, a clear distinction exists now between curves associated to the bell shape and those of the singular branch. Along the bell shape, T_{mid} increases rapidly on reducing p from p_{c2} to $p_{\mathrm{opt}}=0.16$ (by a factor of $\sim1.5-2$). Saturation seems to occur for lower p values a little above 60 K. Along the singular branch, T_{mid} also increases on decreasing p but changes are less marked ($\sim1/3$). Globally, $T_{\mathrm{mid}}(p)$ mimics the superconducting diagram in the vicinity of its bifurcation [Fig. 3(b)].

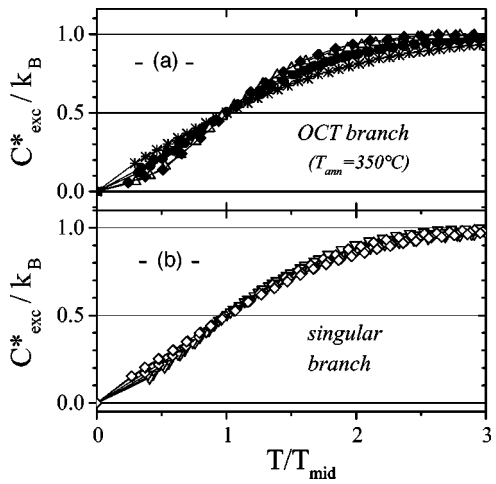

FIG. 4. Normalized specific heat C^{*}_{exc}/k_B, of dragging excitations as a function of the reduced temperature T/T_{mid} (a) for the OCT branch and $T_{an}=350\,^{\circ}C$ and (b) for the singular branch. Same symbols as in Fig. 1.

Consider next the detailed changes in $C^*_{exc}(T)/k_B$ induced by varying p as shown in Fig. 4 as a function of T/T_{mid}. Curves in Fig. 4(a) correspond to the OCT case. Increasing the hole doping leads to a rearrangement in $C^*_{exc}(T)$, marked by a reduced contribution for $T<T_{mid}$ and an increase above. Assuming minor effect from a possible filtering bias (see above) a rearrangement would imply some plasticity in the excitation spectrum by doping. Specifically, less low-lying energy modes are present in the overdoped regime. By contrast, curves from the singular branch [Fig. 4(b)] are hardly modified by varying p. This could reflect a greater rigidity in the excitation spectrum and distinguishes again between the singular branch and the generic cuprate curve.

The present paper shows that the TEP of $Bi_2(Sr_{2-y}La_y)CuO_{6+\delta}$ follows reasonably well the general trend evidenced by OCT for cuprates, except for a singular branch presumably linked to crystalline microdefects over a limited range of La concentration. The $S(T)$ dependence in the normal state is unveiled over a large absolute T range for the underdoped, overdoped and optimal doping regions. The observed sequence of curves supports a drag mechanism with, in particular, the positive steplike form anticipated by Trodahl.[7] Provided some assumptions, a more quantitative analysis, based on a simplified diffusion plus drag model, has been carried out. Within this frame, the effective number of dragging excitation modes decreases linearly with p and finally vanishes in the overdoped region, very close to the critical doping at which superconductivity is suppressed. Differences between the generic OCT curve and the singular branch have also been evidenced and could be associated to a greater or lesser doping plasticity of the dragging excitations spectrum (shift of characteristic frequency and frequency narrowing). Finally the present paper puts the question of the very nature of effective dragging excitations in cuprates and their possible link with HT_c superconductivity.

*Author to whom correspondence should be addressed. Electronic address: Yves.Dumont@ens-phys.uvsq.fr

[1] S.D. Obertelli, J.R. Cooper, and J.L. Tallon, Phys. Rev. B **46**, 14 928 (1992).
[2] J.L. Tallon, J.R. Cooper, P.S.I.P.N. de Silva, G.V.M. Williams, and J.W. Loram, Phys. Rev. Lett. **75**, 4114 (1995).
[3] J.R. Cooper and J.W. Loram, J. Phys. I **6**, 2237 (1996).
[4] D.M. Newns, C.C. Tsuei, R.P. Huebener, P.J.M. van Bentum, P.C. Pattnaik, and C.C. Chi, Phys. Rev. Lett. **73**, 1695 (1994).
[5] G. Hildebrand, T.J. Hagenaars, W. Hanke, S. Grabowski, and J. Schmalian *et al.*, Phys. Rev. B **56**, R4317 (1997).
[6] J.S. Zhou and J.B. Goodenough, Phys. Rev. B **51**, 3104 (1995).
[7] H.J. Trodhal, Phys. Rev. B **51**, 6175 (1995).
[8] B. Sales and B. Chakoumakos, Phys. Rev. B **43**, 12 994 (1991).
[9] H. Zandbergen, W. Groen, F. Fukutomi, and T. Asano, Physica C **156**, 325 (1988); A. Maeda, M. Hase, I. Tsukada, K. Noda, S. Takebayashi, and K. Uchinokura, Phys. Rev. B **41**, 6418 (1990).
[10] Y. Dumont, C. Ayache, A. Carrington, G. Collin, S. Megtert, and A.P. Mackenzie, Physica C **235-240**, 1515 (1994).
[11] Y. Dumont, Ph.D. thesis, Paris-XI, Orsay, 1996.
[12] Y. Dumont and A.P. Mackenzie (unpublished).
[13] L. Vasiliu-Doloc, A.H. Moudden, G. Collin, and J. Doucet, J. Phys. IV **2-3**, 141 (1993); L. Vasiliu-Doloc, Ph.D. thesis, Paris-XI, Orsay, 1995.
[14] G. Collin and Y. Dumont (unpublished).
[15] A.B. Kaiser and C. Uher, *Studies of High Temperature Superconductors*, edited by A.V. Narlikar (Nova Science, New York, 1991), Vol. 7, p. 353
[16] C.K. Subramaniam, C.V.N. Rao, A.B. Kaiser, H.J. Trodahl, A. Mawdsley, N.E. Flower, and J.L. Tallon, Supercond. Sci. Technol. **7**, 30 (1994).
[17] Mu-Yong Choi and J.S. Kim, Phys. Rev. B **59**, 192 (1999).
[18] J.M. Ziman, *Electrons and Phonons* (Clarendon Press, Oxford, 1962), p. 409.
[19] J.P. Jay-Gerin and R. Maynard, J. Low Temp. Phys. **3**, 377 (1970).